IEICE Communications Express, Vol.13, No.3, 68–71

ComEX

LETTER

Non-integer power of two QAM signaling for flexible and nonlinearity tolerant optical fiber transmission systems

Wataru Imajuku[1, a)], **Shunsuke Takahashi**[1], **Yuto Nakamura**[1], **and Ryo Akahoshi**[1]

Abstract This paper studies non-integer power of two-ary quadrature amplitude modulation (QAM) for long-haul optical fiber transmission systems. Numerical simulations show that 12-QAM and 24-QAM provide intermediate solutions on reachable transmission distances among traditional M-QAM such as C8-QAM, 16-QAM, and 32-QAM. In addition, short block length probabilistic shaping of 24-QAM not only provides an intermediate solution with nonlinear tolerance, but also yields greater transmission distances than 16-QAM for the same information data rates.

Keywords: quadrature amplitude modulation, probabilistic shaping, fiber nonlinearity

Classification: Fundamental theories for communications

1. Introduction

Research on increasing the system flexibility of long-haul optical transmission systems has become increasingly important for enhancing cost effectiveness. Recent studies on probabilistic amplitude shaping (PAS) on forward error correction (FEC) platforms have opened new approaches to extending both spectrum efficiency and flexibility in optimizing system capacity and transmission distance in long-haul transmission systems [1]. Recent experiments have demonstrated long-haul transmission over 3,840 km with 168-GBaud probabilistic shaped (PS) 16-QAM signals and over 1,280 km with 168 GBaud PS-36-QAM on the same system infrastructure [2].

However, the shaping gain of PAS is vulnerable to fiber nonlinearity, because PAS increases the peak-to-average power ratio (PAPR) of M-QAM signals. Also, it has been pointed out that the longer probabilistically shaped symbol frames generated by the distribution matcher suffer nonlinear degradation more readily due to the existence of longer successive symbols, as these induce intraband nonlinear interaction when transiting dispersive transmission fiber lines [3]. Recent studies have proposed the use of shorter frames to decrease power spectral density in the low-frequency region [3, 4].

This paper proposes an additional scheme to enhance both the flexibility and nonlinear tolerance of long-haul transmission systems by employing non-integer powers of two M-QAM constellation templates [5] and two-dimensional probabilistic amplitude-phase shaping over non-binary Forward Error Correction (FEC) platforms [6, 7]. Specifically, our numerical simulations compare the reachable distances of PS-12-QAM and PS-24-QAM signals with those of C8-QAM [8], 12-QAM, 16-QAM, PS-16-QAM, 24-QAM, 32-QAM, and PS-36-QAM signals. In the simulations, we employ Normalized Mutual Information (NMI) as the performance metric, since this metric is known to be an excellent performance predictor for systems employing symbol metric soft decoders [9].

2. Encoding for non-integer powers of two QAM signaling

The system model in Fig. 1(a) is basically identical to the model proposed in [6, 7], which enables probabilistic amplitude shaping (PAS) to be employed on NB-LDPC platforms [10, 11, 12]. This paper modifies the model to generate two-dimensional probabilistically shaped n amplitude-phase symbols with M/4 signal points. Namely, the input information bit stream is divided into amplitude-phase modulation (APM) bits and quadrant modulation (QDM) bits. Here, the k APM- bits are mapped to n amplitude-phase symbols and non-binary n/l code words, while QDM-bits are mapped

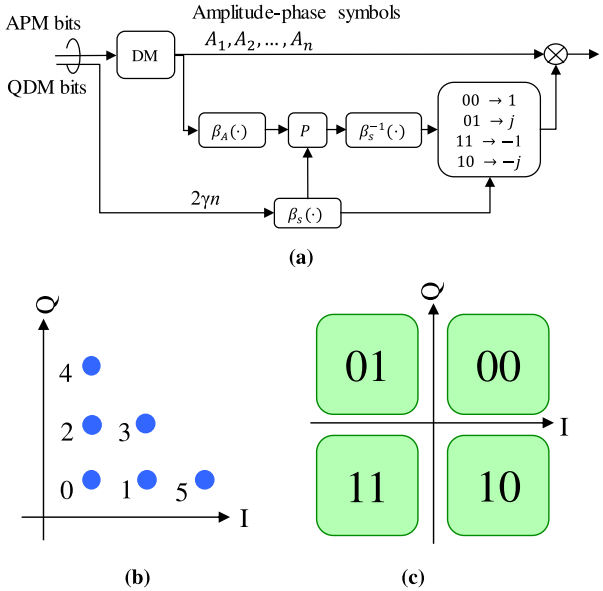

Fig. 1 System model to support non-integer powers of two QAM constellation signaling, (a) configuration of PAS over NB-LDPC encoder proposed in [6], (b) signal points of amplitude-phase symbols and (c) defined quadrant bits to support two-dimensional PAS.

[1] Department of Humanity-Oriented Science and Technology, Kindai University, Iizuka, Fukuoka, 820-8555 Japan

[a)] imajuku@ieee.org

DOI: 10.23919/comex.2023XBL0166
Received November 28, 2023
Accepted December 12, 2023
Publicized January 15, 2024
Copyedited March 1, 2024

to the quadrant of amplitude-phase symbols along with a parity-check code word. For example, consider the case of 24-QAM constellation signaling with GF(q = 8) code-words. The distribution matcher generates four amplitude-phase symbols with 6(= 24/4) signal points from the eight information bits input as shown in Fig. 1 (b). Each two amplitude-phase symbol generated is mapped to a corresponding GF(q = 8) code word, where the order of Galois Field might be q = 7, which is the minimum prime number over the total summation of signal points for all two amplitude-phase symbols. On the other hand, $2\gamma n$ bits of the information bits are assigned as the part of the QDM bits and the other parts of the QDM bits are assigned by parity check bits derived from all input information bits. Then, all QDM bits assign the quadrants of the amplitude-phase symbols as shown in Fig. 1(c), where γ is the ratio of information bits among all QDM bits used to assign the quadrants of the amplitude-phase symbols. Thus, the system transmits three code-word symbols encoded with GF(q = 8) (or GF(q = 7)) for every four 24-QAM symbols.

This paper assumes 12-QAM and 24-QAM constellations without outer signal points of 16-QAM and 32-QAM constellations, respectively, as shown in Fig. 2(a) and (b). Figure 2(c) shows Mutual information (MI) rates as a function of signal-to-noise ratio (SNR) of 12-QAM, PS-12-QAM, 24-QAM and PS-24-QAM signals along with other M-QAM signals simulated in this study. The evaluated PS-M-QAM signals were formed as concise frames with lengths of four symbols by utilizing a small look-up table. The APM-bits were mapped to four amplitude-phase symbols, while QDM-bits were mapped to the quadrant of those symbols. The frames composed of PS-12-QAM and PS-24-QAM symbols realize spectrum efficiency of 3 bit/symbol and 4 bit/symbol which are the same with those of C8-QAM [8] and 16-QAM signals, respectively. Here, we have to note that the C8-QAM symbols can achieve higher MI rates than those of 8PSK if normalized MI rates are higher than about 0.7. On the other hand, the frames composed of PS-16-QAM and PS-36-QAM symbols realize spectrum efficiency of 3.5 bit/symbol and 4.5 bit/symbol, which match those of 12QAM and 24-QAM signals, respectively.

In the high SNR region, the MI rates of the PS-12-QAM, PS-16-QAM, PS-24-QAM, and PS-36-QAM were reduced to 3.26, 3.78, 4.15 and 4.78 bit/symbol, respectively, while those without probabilistic shaping were 3.58, 4.0, 4,58 and 5 bit/symbol, respectively. Critically, PS-12-QAM and PS-24-QAM have higher MIs in low SNR conditions by approaching Shannon's channel capacity limit. PS-12-QAM and PS-24-QAM signals having the same spectrum efficiency as C8-QAM and 16-QAM have shaping gains of 0.2 dB and 0.4 dB at their MI rate conditions of 2.55 bit/symbol and 3.40 bit/symbol, respectively, which are 85% of their maximum MI rates. This helps to yield reachable transmission distances for PS-12-QAM and PS-24-QAM signals that exceed those of conventional C8-QAM and 16-QAM signals.

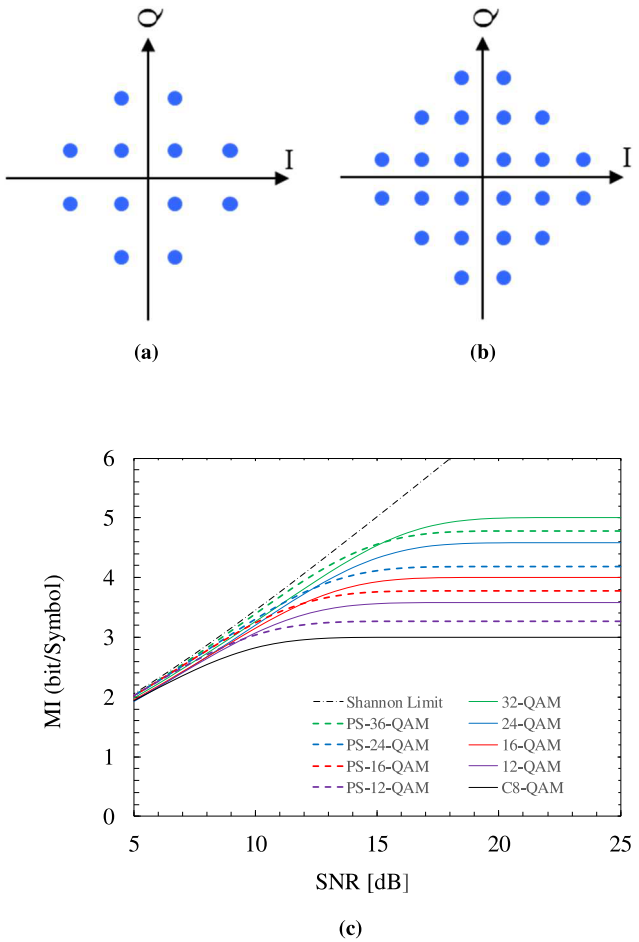

Fig. 2 Constellation diagram of (a) (PS)-12-QAM and (b) (PS)-24-QAM, and mutual information rates of PS-12-QAM, PS-16-QAM, PS-24-QAM and PS-36-QAM in comparison with C8-QAM, 12-QAM, 16-QAM, 24-QAM, and 32-QAM as a function of SNRs.

3. Simulation and results

We simulated the transmission performance of polarization multiplexed optical pulses at a rate of 175 GBaud per channel as shown in Fig. 3. At the transmitter, pseudo-random bit streams (PRBS) with the length of $2^{15} - 1$ were iteratively generated and mapped to 180,000 complex symbols via the distribution matcher in the case of probabilistic shaping. The

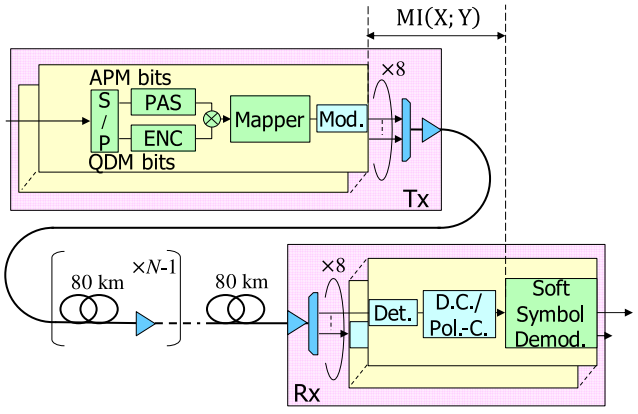

Fig. 3 Simulation model employed in this study. Input data of $2^{15} - 1$ PRBS are divided to APM bits and QDM bits. In this simulation, QDM bits were simply mapped to quadrants and multiplied to the output of PAS module. The received optical signals are electrically compensated by dispersion compensator (D.C.) and polarization compensator (Pol.-C.).

pulses were filtered by a root-raised-cosine (RRC) filter with a roll-off factor of 0.1. Those signals were then multiplexed with 200 GHz spacing without optical filtering to form 8 channel wavelength division multiplexed links. We set a post-optical amplifier at the output of the transmitter with noise figure of 6 dB. The length of each span was assumed to be 80 km with loss coefficient of $\alpha = -0.160$ dB/km, dispersion parameter of $\beta_2 = -21.8$ ps^2/km, $\beta_3 = 0.114$ ps^3/km, and nonlinear coefficient of $\gamma = 0.600$ W^{-1}km^{-1} ; all values were incorporated to the nonlinear Manakov equation for each split-step Fourier section with step size of 50 m. We also simulated polarization mode dispersion. The mean differential group delay of DGD = 0.2 ps/km$^{0.5}$ was assumed, while the value in each section randomly varied with the standard deviation of 20% of the mean value. In this paper, we defined the NMI as

$$\mathrm{NMI}(X;Y) = \mathrm{MI}(X;Y)/\mathrm{H}(X) \quad , \tag{1}$$

and utilized Eq. (1) as the performance metric assuming symbol metric soft decoding.

Figure 4 (a) shows the NMI rates of non-PS signals such as 12-QAM, 24-QAM signals along with those of conventional M-QAM signals at 2,000 km transmission distance as a function of launch power per wavelength-channel. Similarly, Figure 4 (b) shows the NMI rates of PS signals such as PS-12-QAM and PS-24-QAM signals along with those of conventional PS-M-QAM signals in the same conditions as Fig. 4 (a). The NMI rates peak at around 1 dBm, which is determined by both effects of Additive White Gaussian Noise (AWGN) and nonlinear degradation of waveforms. The NMI rates of 12-QAM signals is intermediate between those of C8-QAM and 16-QAM signals. The NMI rate of 24-QAM signals is intermediate between those of 16-QAM and 32-QAM signals. Specifically, the NMI rates of 24-QAM signals are closer to those of 16-QAM signals rather than 32-QAM signals.

Similarly, the NMI rates of PS-24-QAM signals show excellent performance, specifically under the high launch power condition. The NMI rates of PS-24-QAM not only provide an intermediate solution between PS-16-QAM and PS-36-QAM, but they also match those of PS-16-QAM under high launch power conditions. Thus, PS-24-QAM provides excellent nonlinearity-tolerant performance in long haul transmission systems. On the other hand, it is clarified that the NMI rates of PS-12-QAM having the same spectrum efficiency as C8-QAM cannot match those of C8-QAM.

Figure 5 plots transmission distance in the condition of optimized average launch power per channel of 1 dBm for each modulation scheme. The broken line shows NMI of 0.85, which represents the post-soft decision FEC bit error rate of 10^{-4} with code rate of 0.8 [9]. This figure clearly shows that the error free distance decreases more steeply as the M-QAM constellation cardinality increases. The reachable transmission distance with NMI above 0.85 of the C8-QAM signals is 6,080 km, while 16-QAM and 32-QAM signals achieve 3,200 km and 1,760 km, respectively. On the other hand, the 12-QAM and 24-QAM signals reach 3,840 km and 2,400 km, respectively, which are intermediate distances among conventional M-QAM signals.

As for PS signals, the reachable transmission distance

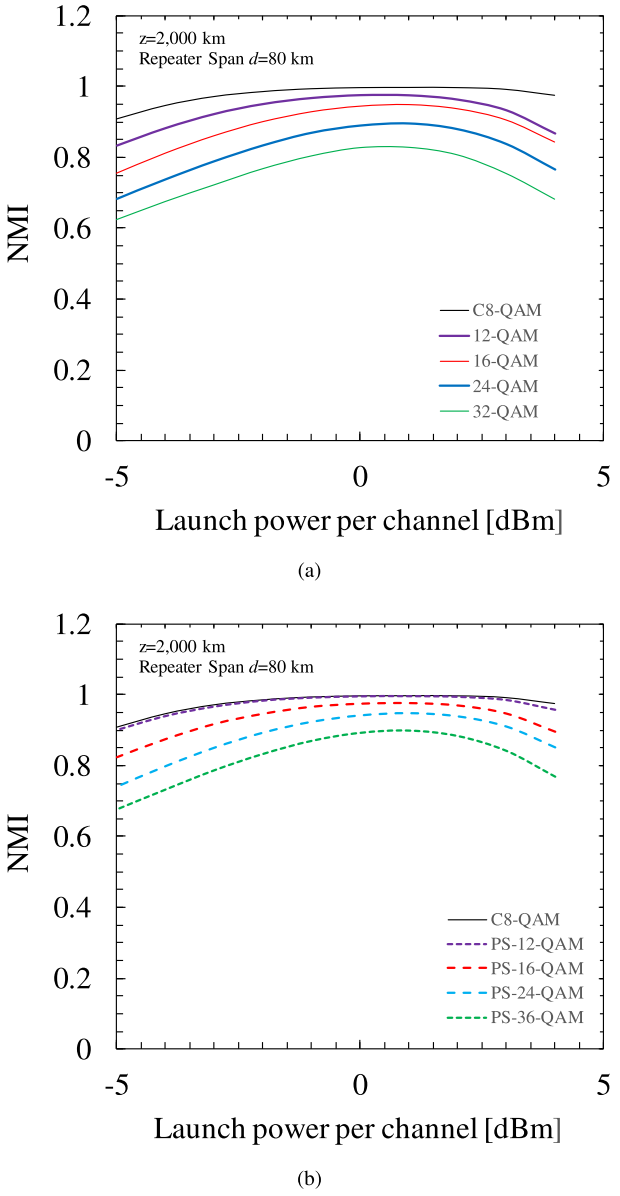

Fig. 4 The NMI rates of (a) non-PS and (b) PS signals of 12-QAM, 16-QAM, 24-QAM, 32(36)-QAM as a function of average launch power per wavelength-channel. The NMI rates of C8-QAM are also plotted as a reference in both figures.

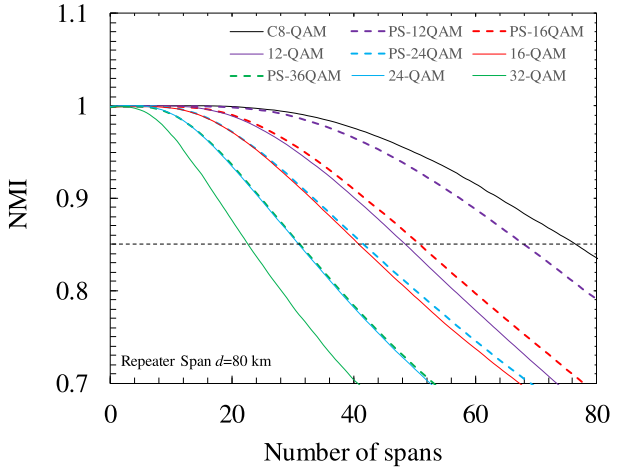

Fig. 5 The NMI rates of non-PS and PS signals as a function of transmission distance. The average launch power of each signal is 1 dBm.

of PS-12-QAM signals does not match that of C8-QAM signals. If the spectrum efficiency is to be 3 bit/symbol, C8-QAM seems the best solution for achieving longer distances. We believe this result originates from the near constant modulus format of C8-QAM, which also offers robustness to nonlinear degradation. On the other hand, the PS-24-QAM signals reach 3,280 km, which is 800 km longer than that of PS-36-QAM signals and 720 km shorter than that of PS-16-QAM signals. Also, we have to note that the PS-24-QAM signals reach 80 km further than 16-QAM signals, while realizing the same spectrum efficiency. Thus, non-integer power of two signaling such as 12-QAM, 24-QAM, and PS-24-QAM provide intermediate reachable distances in long-haul transmission systems.

4. Conclusion

This paper proposes an innovative scheme to enhance both the flexibility and nonlinear tolerance of long-haul transmission systems by employing non-integer powers of two M-QAM constellation templates and two-dimensional probabilistic amplitude-phase shaping. This paper demonstrated that 12-QAM, 24-QAM, and PS-24-QAM signals offer intermediate solutions among the traditional modulation schemes in the view point of the NMI rates. Specifically, we note that the NMI rates of PS-24-QAM signals match those of PS-16-QAM signals under the high signal power condition, which indicates PS-24-QAM signals are tolerant against fiber nonlinearity. Also, PS-24-QAM signals offer longer transmission distances than 16-QAM signals, while realizing the same spectrum efficiency. Thus, the non-integer powers of two QAM scheme provides a new methodology for creating better combinations of system capacities and transmission distances in long-haul transmission systems.

Acknowledgments

This research is supported by the ICT priority technology R&D promotion of innovative optical transmission technologies for supporting green society project (JMPI00316) funded by the Ministry of Internal Affairs and Communications Japan. The authors thank Prof. Keisuke Kasai, Tohoku University for the advice on receiver filters. The authors should note that this study has been supported by Prof. Hiroshi Shiratsuchi and Prof. Takanori Matsuzaki, Department of Humanity-Oriented Science and Technology Kindai University through their continuous assistance in arranging the research environment. Lastly, the authors thank editors and reviewers for giving us valuable comments on improving this paper.

References

[1] G. Böcherer, F. Steiner, and P. Schulte, "Bandwidth efficient and rate-matched low-density parity-check coded modulation," *IEEE Trans. Commun.*, vol. 63, no. 12, pp. 4651–4665, 2015. DOI: 10.1109/TCOMM.2015.2494016

[2] M. Nakamura, T. Sasai, K. Saito, F. Hamaoka, T. Kobayashi, H. Yamazaki, M. Nagatani, Y. Ogiso, H. Wakita, Y. Kisaka, and Y. Miyamoto, "1.0-Tb/s/λ 3840-km and 1.2-Tb/s/λ 1280-km transmissions with 168-GBaud PCS-QAM signals based on AMUX integrated frontend module," Proc. OFC2022, W3C.1, 2022. DOI: 10.1364/OFC.2022.W3C.1

[3] W.-R. Peng, A. Li, Q. Guo, Y. Cui, and Y. Bai, "Transmission method of improved fiber nonlinearity tolerance for probabilistic amplitude shaping," Title of paper in proceeding, *IEEE Commun. Lett.*, vol. 28, no. 20, pp. 29430–29441, 2020. DOI: 10.1364/OE.400549

[4] T. Fehenberger, D.S. Millar, T. Koike-Akino, K. Kojima, K. Parsons, and H. Griesser, "Analysis of nonlinear fiber interactions for finite-length constant-composition sequences," *J. Lightw. Technol.*, vol. 38, no. 2, pp. 457–465, 2020. DOI: 10.1109/JLT.2019.2937926

[5] S. Noda, Y. Saito, and T. Yoshida, "Study on configuration and error ratio performance of M-QAM whose number of signal points is not a power of 2," IEICE Trans. Commun. (Japanese Edition), vol. J88–B, no. 5, pp. 921–932, 2005.

[6] F. Steiner, G. Livay, and G. Böcherer, "Ultra-sparse non-binary LDPC codes for probabilistic amplitude shaping," Proc. IEEE Global Telecom. Conf. (GLOBECOM), pp. 1–5, Dec. 2017. DOI: 10.1109/GLOCOM.2017.8254155

[7] F. Steiner, G. Böcherer, and G. Livay, "Bit-metric decoding of non-binary LDPC codes with probabilistic amplitude shaping," *IEEE Commun. Lett.*, vol. 22, no. 11, pp. 2210–2213, 2018. DOI: 10.1109/LCOMM.2018.2870180

[8] K. Kojima, T. Koike-Akino, D.S. Millar and K. Parsons, "BICM capacity analysis of 8QAM-alternative modulation formats in nonlinear fiber transmission," Tyrrhenian International Workshop on Digital Communications (TIWDC), pp. 57–60, 2015. DOI: 10.1109/TIWDC.2015.7323337

[9] L. Schmalen, A. Alvarado, and R. R.-Müller, "Performance prediction of nonlinearity error correction in optical transmission experiments," *J. Lightw. Technol.*, vol. 35, no. 4, pp. 1015–1027, 2017. DOI: 10.1109/JLT. 2016.2609932

[10] D. Declercq and M. Fossorier, "Decoding algorithms for nonbinary LDPC codes over GF(q)," *IEEE Trans. Commun.*, vol. 55, no. 4, pp. 633–643, 2007. DOI: 10.1109/TCOMM.2007.894088

[11] M. Arabaci, I.B. Djordjevic, R. Saunders, and R.M. Marcoccia, "High-rate nonbinary regular quasi-cyclic LDPC codes for optical communications," *J. Lightw. Technol.*, vol. 27, no. 23, pp. 5261–5267, 2009. DOI: 10.1109/ JLT.2009.2029062

[12] T. Koike-Akino, K. Sugihara, D.S. Millar, M. Pajovic, W. Matsumoto, A. Alvarado, R. Maher, D. Lavery, M. Paskov, K. Kojima, K. Parsons, B.C. Thomsen, S.J. Savory4, and P. Bayvel, "Experimental demonstration of nonbinary LDPC convolutional codes for DP-64QAM/256QAM," ECOC'16, We1.C.5, 2016.